Preprints of the 21st IFAC World Congress (Virtual)
Berlin, Germany, July 12-17, 2020

Exploiting Bend-Twist Coupling in Wind Turbine Control for Load Reduction ⋆

Marcus Wiens * **Tobias Meyer** * **Jan Wenske** *

* *Fraunhofer Institute for Wind Energy Systems IWES, Am Luneort 100, 27572 Bremerhaven, Germany (e-mail: marcus.wiens@iwes.fraunhofer.de)*

Abstract: The ever-increasing dimensions of wind turbines are associated with higher structural loads. Therefore, there is a demand for advanced load reduction techniques. In the design of rotor blades, the bend-twist coupling effect is used for passive load reduction. This research shows how this effect can be augmented with active load reduction through controls that exploit bend-twist coupling. The twist rate of the rotor blades is utilized for gust detection. In addition to regular closed-loop pitch control, the twist rate is used to adjust the collective pitch angle using feedforward control. Extreme loads for flap-wise bending moment can be reduced on average by up to 6 % and tower acceleration is reduced by 15 %. Overall, this method is suitable for reducing extreme loads while maintaining fatigue damage compared to the reference case.

Keywords: Wind Turbine Control, Bend Twist Coupling, Load Reduction, Peak Minimization, Gust Detection

1. INTRODUCTION

Larger wind turbines demand efficient methods for load reduction. The wind turbine loads are mainly dependent upon the wind speed. Loads increase with the height of the wind turbine due to the higher wind speeds. With the increasing size of the rotor, the wind speeds across the rotor plane are more unevenly distributed due to wind shear. This leads to increased structural loads. Consequently, much research is focused on mitigating loads. Therefore, all aspects of a wind turbine, such as the materials of the wind turbine itself, the structural design and the controller, are continuously optimized (van Kuik, G. A. M. et al. (2016)).

1.1 Wind Turbine Control

A main influence on the wind turbine loads is established by the control algorithm. Thus, there is a need for load reducing control algorithms to protect and extend the lifetime of the wind turbines. One common approach for load reduction control is established by individual pitch control (IPC), see Bossanyi (2003). The load reduction is achieved by adjusting each pitch angle individually. In this way, the uneven load distribution is mitigated. Active damping by modifying the generator torque is used to reduce torsional vibrations in the drive train (Burton et al. (2011)). Model predictive control is another advanced concept for wind turbine control and currently the topic of many studies (e.g. Njiri and Söffker (2016)). Other advanced control strategies like repetitive control by Navalkar et al. (2014) also significantly reduce loads.

⋆ This research was carried out in the scope of the SmartBlades2 project (0325601A/B/C/D), funded by the German Federal Ministry for Economic Affairs and Energy (BMWi) based on a decision of the Parliament of the Federal Republic of Germany.

1.2 Bend-Twist Coupling

A design goal for rotor blades is the reduction of structural loads. One way to achieve significantly reduced loads is to couple the axial bending of the blades with their structural twist. This effect is called Bend-Twist-Coupling (BTC). If a rotor blade has BTC properties, it will twist when the rotor blade is under load. Realizations of BTC include geometric BTC and structural BTC using swept blades or a dedicated layup of the composite material, respectively. Structural BTC leads to anisotropic material properties. In this study, geometric BTC is employed by sweeping the blade. A regular blade is mostly straight along the pitch axis, while a swept blade is offset at the tip. This way, wind force will create a twisting moment around the pitch axis. This will lead to increased torsion of the rotor blade, if the blade is under heavy load due to high wind speeds. As a consequence, the angle of attack of the blade is reduced, which in turn reduces load. An overview of previous studies is given by Stäblein et al. (2017b) and they also perform an intensive study on the aeroelastic properties of BTC blades. It is shown, that flutter speed is reduced for flap-twist coupling. Kallesøe (2011) analyzes the stability of swept blades and shows that a flap-wise excitation and corresponding deflection also leads to an edge-wise deflection and torsion along the blade axis.

Advanced studies with BTC rotor blades regarding wind turbine control found a potential for additional load reduction. The NREL 5 MW wind turbine is studied with swept blades in Verelst and Larsen (2010). It is found that flap-wise fatigue and extreme loads are reduced. But a different sweep shape is suggested to counteract high torsional moments in the blade root. Modal properties and stability of the DTU 10 MW wind turbine is analyzed by Stäblein et al. (2017a). They find that stability is affected differently by the type of BTC (flap- or edge-

twist). Bottasso et al. (2012) perform an optimization of the blade sweep and also combined BTC rotor blades with IPC. A synergistic load reduction effect is identified. In a recent study, Manolas et al. (2018) use active control with BTC. By adjusting the pitch angle and trailing edge flaps individually, a benefit for load reduction is shown. Another suggestion is made with the use of a plasma actuator to reduce lift during gust events for load reduction, as Liu et al. (2018) showed. However, additional actuators increase the technical complexity. Therefore, this study investigates how the active use of BTC effect can be further exploited by a novel feedforward control loop.

1.3 Outline of this Work

In Section 2, our simulation setup and the feedforward control loop are presented. The impact on the wind turbine behavior is shown in Section 3. Findings are discussed in Section 4 and conclusion is given in Section 5.

2. METHODS

All simulations are based on a full aeroelastic wind turbine model. In addition, a baseline control is used as reference for evaluation of the load reduction effect.

2.1 Simulation Setup and Reference Controls

In our work, we use a generic aeroelastic wind turbine model created in Modelica for Wind Turbines (MoWiT), see Thomas et al. (2014). This wind turbine model has a high accuracy and can be compared to GH Bladed, see Leimeister and Thomas (2017). GH Bladed is a well known tool in wind energy industry. MoWiT makes use of the modal reduction technique and provides various detailed aeroelastic models, including Blade Element Momentum Theory (BEM) or Generalized Dynamic Wake (GDW). The tower and rotor blades are flexible structures constructed of single three-dimensional beam elements.

The generic, three-bladed, horizontal axis, direct-drive wind turbine model, known as IWT 7.5 MW-164, is applied in this study. A verification of the wind turbine model is performed by Popko et al. (2018). The wind turbine is modeled by approximately 80000 equations in MoWiT. This wind turbine model is designed for IEC Class 1 (IEC (2019)) wind conditions. The hub height is 120 m and the rotor blades have a length of 80 m. The tower is modeled by 9 and the rotor blade by 31 beam elements. We set the IWT 7.5 MW-164 with straight blades and baseline controller as the reference (Base) in this study. It is compared against a passive configuration with BTC blades and two active configurations. A description of the blade sweep can be found in Section 2.2. The first active configuration combines BTC blades with individual pitch control (IPC) and the second configuration uses BTC with the presented novel control method collective twist control (CTC) from Section 2.4. This gives a total of four configurations:

(1) Straight rotor blade (Base).
(2) BTC rotor blades (BTC).
(3) BTC rotor blades with IPC (IPC).
(4) BTC rotor blades with CTC (CTC).

The simulation setup is established as a closed-loop system. A baseline controller for IWT 7.5 MW-164 is designed with Simulink (MATLAB 2017b) and a DLL is generated by MATLABs code generation function. Afterwards, the DLL is integrated into the MoWiT model to obtain a closed-loop simulation setup. The design of the baseline controller corresponds to (Njiri and Söffker, 2016, p. 379). For Region 2, the $k \cdot \omega^2$-law is applied for torque control. In Region 3, the torque is constant at rated value and a gain-scheduled PI controller maintains the rotor speed by adjusting the pitch angle. The collective pitch angle β_{PI} is determined from the generator speed error $\omega - \omega_0$, where ω_0 is the rated generator speed. A notch filter prevents excitation of the 1$^{\text{st}}$ tower eigenfrequency. Additionally, IPC is implemented as two separate PI controllers for vertical and horizontal imbalance. Poles are placed to find a suitable trade off between tracking error and induced loads. Due to the changes in aerodynamics, the wind turbine with BTC blades requires adjusted controller gains to obtain equal control action. The gains are adjusted so, that both controllers have the same poles. In this way, comparability is maintained.

2.2 Bend-Twist Coupled Rotor Blade

The straight rotor blade of the IWT 7.5 MW-164 has a pre-bend and is designed without sweep. For the investigated wind turbine model, a swept rotor blade has been designed in the Smart Blades project (Teßmer et al. (2016)). In MoWiT, the shape of the rotor blade is determined by a reference line. It is defined as the line that connects all center points of each element's chord length along the rotor blade. Correspondingly, the airfoils of the rotor blade are positioned around this reference line at certain nodes. Each node represents a beam element. A sweep can be added to the blade shape by changing the coordinates of the reference line. The shift is performed so that all the element nodes remain on the same radius as the straight reference blade. Thus, the total rotor radius remains constant. This is done to minimize the differences between the rotor blade designs and thereby increase their comparability. The shift amount is defined by the sweep function, which is obtained from the underlying study as

$$y_{\text{sweep}} = \begin{cases} y_{\max}\left(\dfrac{x - x_{0s}}{x_{\text{tip}} - x_{0s}}\right)^3 & \text{if } x_{0s} \leq x \leq x_{\text{tip}} \\ 0 & \text{else.} \end{cases} \quad (1)$$

According to the underlying study, the sweep is applied in trailing edge direction, which results in a twist-to-feather configuration. The sweep start x_{0s} is 60 m from the blade root and the maximum sweep $y_{\max}$ at blade tip x_{tip} is set to 2 m. The reference lines of the straight and swept rotor blade are compared in Figure 1. In order to reduce maximum loads, but unvarying fatigue loads, the blade is designed as presented. The underlying sweep design parameters are published in Teßmer et al. (2016). In this study, the rotor blade design is not further optimized to provide equal energy extraction from the wind. The influences of that are discussed shortly. We compare the aerodynamic properties of the rigid straight and swept blades. They show similar aerodynamics indicated by similar c_p-curves. In simulations with higher fidelity, the rotor blade is flexible and therefore, a change in aerodynamics

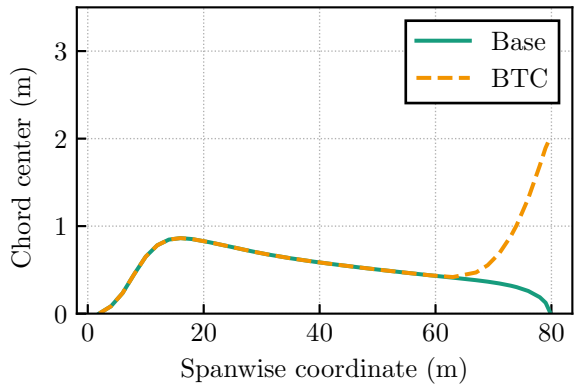

Fig. 1. Comparison of the reference base rotor blade (Base) and swept rotor blade (BTC)

and correspondingly power production is expected. It is assumed that this occurs due to the increased twisting of the BTC blades. This results in a different angle of attack for certain wind speeds. Aerodynamic inflow is probably not optimal in this case. One possibility for resolving this is also to change the pre-twist of the rotor blade.

2.3 Identification of BTC-Specific Measures

Simulations of the wind turbine with BTC rotor blades show that the BTC configuration is more sensitive to rapid changes in the wind. We assume that the twist rate at the blade tip can be used in a controller. In terms of this study, the twist rate is defined relative to the pitch angle. The rotation of the blade tip $\dot{\vartheta}_{\text{tip}}$ consists of the pitch movement $\dot{\beta}_{\text{PI}}$ and the twist rate $\dot{\vartheta}$ as

$$\dot{\vartheta}_{\text{tip}} = \dot{\beta}_{\text{PI}} + \dot{\vartheta}. \tag{2}$$

A few simulations are conducted to determine how fast different components respond to a gust of wind. Figure 2 shows the normalized responses of different components to a step in wind speed from 14 m/s to 17 m/s at 50 s. The twist rate shows a fast reaction for the Base and BTC configuration. A more direct response is observed for the BTC twist rate after the step change. The bending moments (BM) increase immediately, due to the sudden change in wind speed. Other components such as rotor speed or tower top deflection (dflc.) show higher inertia. This indicates that the twist rate is a suitable measure for rapid wind speed changes. An inertial measurement unit (IMU) at the blade tip could establish a measurement of the twist rate. Alternatively, multiple IMUs placed along the rotor blade combined with an observer model could be used to estimate the blade twist rate.

2.4 Feedforward Twist Controller Design

Feedforward control is commonly used in wind turbine control, see Njiri and Söffker (2016). For example, Meng et al. (2016) use an estimator for the effective wind speed to determine a feedforward for the pitch rate. Results show improvements in load reduction. Here, it is proposed to use the twist rate in a feedforward control loop. The high sensitivity of the twist rate to sudden wind speed changes is shown in Figure 2. This characteristic of the blade tip is used to detect gusts and thus opens the possibility for

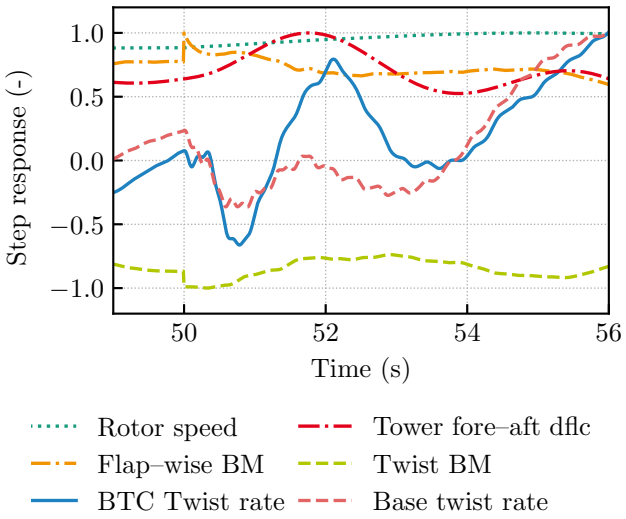

Fig. 2. Normalized component responses of wind turbine with BTC blades to step in wind speed

the controller to react faster to gusts. The twist rate is obtained at the blade tip and fed into a low-pass filter with cutoff frequency at 0.65 Hz to emulate a blade tip sensor. In this way, high fluctuations are removed. The frequency is determined empirically.

The presented collective pitch baseline proportional-integral controller is extended by an additional feedforward control loop. See Figure 3 for the block diagram. The twist rate signals $\dot{\vartheta}_i$ are added up and then multiplied by a gain value K. Its value is determined empirically to $K = 0.5$ to achieve a compromise between effectiveness and the amount of feedforward influence. This gives the following control law for the pitch angle β

$$\begin{aligned}\beta(t) &= K_P \cdot (\omega_0 - \omega(t)) + K_I \cdot \int_0^t (\omega_0 - \omega(\tau))\,\mathrm{d}\tau \\ &\quad + K \cdot \sum_{i=1}^{3} \dot{\vartheta}_i(t).\end{aligned} \tag{3}$$

The filter block is assembled of a low-pass and a notch filter. Thereby, fluctuations above 4 Hz are removed and the notch filter prevents excitation of the blade movement at the 1st eigenfrequency of the flap-wise direction. After all, the signal from the feedforward is limited to $\pm 2\,^\circ$ by the saturation block in order to prevent large changes of the pitch angle. In the case of increasing wind speed, a twisting moment at the blade tip is created, which twists the rotor blade to feather. The rate of the torsion motion at the blade tip is detected by the blade tip sensor. This tip torsion will lead to an increased pitch angle command from the controller. Thereby, the angle of attack is changed faster, resulting in a load reduction. The faster pitch angle adjustment to the changed wind speed reduced the torsion of the rotor blade. For decreasing wind speed, the opposite occurs. This novel control strategy is further referred to as Collective Twist Control (CTC).

2.5 Evaluation

The simulations are performed using Dymola 2019 FD01. For the integration we use the Runge-Kutta-4 algorithm

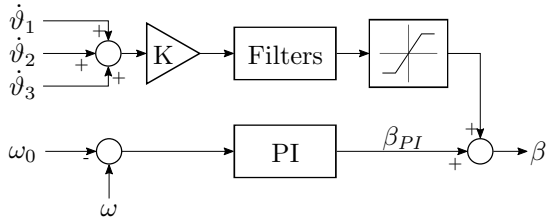

Fig. 3. Block diagram of the feedforward collective twist controller with baseline PI controller

and a fixed time step of 0.01 s. Extreme operating gust (EOG) wind profiles are applied to estimate extreme loads for the wind turbine. The EOGs are designed according to IEC-61400-1 and simulated for single wind speeds in the operating range. Turbulent wind profiles are used to estimate fatigue loads. The wind fields were generated with TurbSim (Jonkman (2009)). Every wind field is generated using different random number generator seeds for each wind speed and yaw angle ($-8\,^\circ$, $0\,^\circ$ and $+8\,^\circ$). The wind speed range spans from cut-in (3 m/s) to cut-out (25 m/s) in steps of 2 m/s. We use six seeds per wind field setting, which gives 216 simulations for each wind turbine configuration. Each simulation is evaluated with damage equivalent load (DEL) calculation (Sutherland (1999)) for the blade root, hub, tower top and bottom. The Wöhler coefficients for the blades are set to 10, others to 3. The outcome is weighted with the Weibull distribution of the wind speed of an IEC class 1 wind site.

3. RESULTS

All simulations were conducted with BEM and GDW as the aeroelastic model, in order to provide a more general statement of the effectiveness of the presented method. For the sake of clarity, only the results from the BEM model are presented in the following, since the large amount of results. Resulting trends and effects exhibit similar behavior. The specific values varied in a range of 5 %.

3.1 Extreme Loads

The effectiveness of CTC is shown in the case of EOG simulations. Here, EOGs are simulated for all wind speeds in the operating range of the wind turbine. Figure 4 presents detailed responses of the different wind turbine configurations in the time domain. The EOG occurs at $t = 50$ s for a wind speed of 15 m/s. When the gust arises, the twist angle of the rotor blade increases due to the higher load. As a result, the pitch angle is adjusted earlier for CTC. In addition, CTC avoids to follow the peak of the EOG and remains at a lower pitch angle between $t = 55$ s and $t = 60$ s. The IPC pitch angle oscillates at $1p$ and is displayed for a single blade only.

The highest influence of CTC on loads is found for the flap-wise bending moment and the tower top acceleration, see Figure 5a and Figure 5b, respectively. The simulation results are presented particularly for wind speeds around the rated wind speed of 12 m/s and a high wind speed at the end of the operating range. The maximum value of the flap-wise bending moment is reduced by all investigated configurations compared with the Base case. Using BTC rotor blades is already beneficial with a reduction of about 9 % in the transition region. This is further improved by using active control methods like IPC and CTC. In fact, CTC leads to the highest absolute reduction in the transition region (12 %) and also to the highest wind distribution averaged reduction of 6 %. Furthermore, CTC is mostly effective for reduction of the tower top acceleration. The maximum reduction of 24 % is achieved for rated wind speed at 12 m/s. For wind speeds around 9 m/s, the passive use of BTC leads to an increased maximum acceleration for the tower top. This negative effect is prevented by the use of CTC such that the maximum acceleration falls 4 % below the value of the base case. Thus, CTC is very effective for reducing the maximum acceleration of the tower top. IPC shows similar reduction potential as passive BTC. Overall, CTC has the highest impact on the maximum loads compared with the other configurations.

All findings regarding EOG are summarized in Table 1, which contains the maximum relative differences of DEL to the Base case. The best results are found for the

Table 1. Changes relative to Base configuration for maximum loads during EOG

Load	BTC	IPC	CTC
Blade root edge-wise moment	1.01	0.99	1.00
Blade root flap-wise moment	0.96	0.96	0.94
Blade root twist moment	1.10	1.08	1.07
Blade tip flap-wise dflc.	0.98	0.97	0.94
Blade tip edge-wise dflc.	0.97	0.94	0.95
Hub force fore-aft	0.96	0.96	0.94
Hub force side-side	0.99	0.90	0.98
Tower bottom fore-aft BM	1.00	0.96	1.01
Tower bottom side-side BM	0.95	0.95	0.91
Tower top fore-aft acc.	0.94	0.93	0.85

tower acceleration (acc.) in fore-aft direction, especially for CTC. Additionally, CTC limits the blade movement to 95 % in flap- and edge-wise direction. This also reduces the flap-wise bending moment. Similarly to the results with turbulent wind, the twist moment at the blade root also increases in simulations with EOG by 10 %. However, active control methods IPC and CTC are able to reduce the increase to 7 %.

A detailed analysis of the aerodynamics is carried out to explain BTC in this setup. It is found that the differences between the rotor blades in lift coefficient and angle of attack are higher at the blade tip than in the middle section. Especially, differences are noticeable for the swept area. For the BTC blades, the inflow conditions are impaired. This reduces the load in the upper blade section and therefore the blade tip deflection. Consequently, the maximum value of the flap-wise bending moment is reduced by all BTC configurations compared to the Base case.

3.2 Turbulent Wind

The results for turbulent wind simulations are presented in Table 2. In this table, the relative changes of DELs with reference to the Base case are listed for different loads and energy production. Overall, the CTC method only has a minor influence on the fatigue loads. The only drawback is found for the tower bottom bending moment in fore-aft direction, which is increased for all analyzed configurations

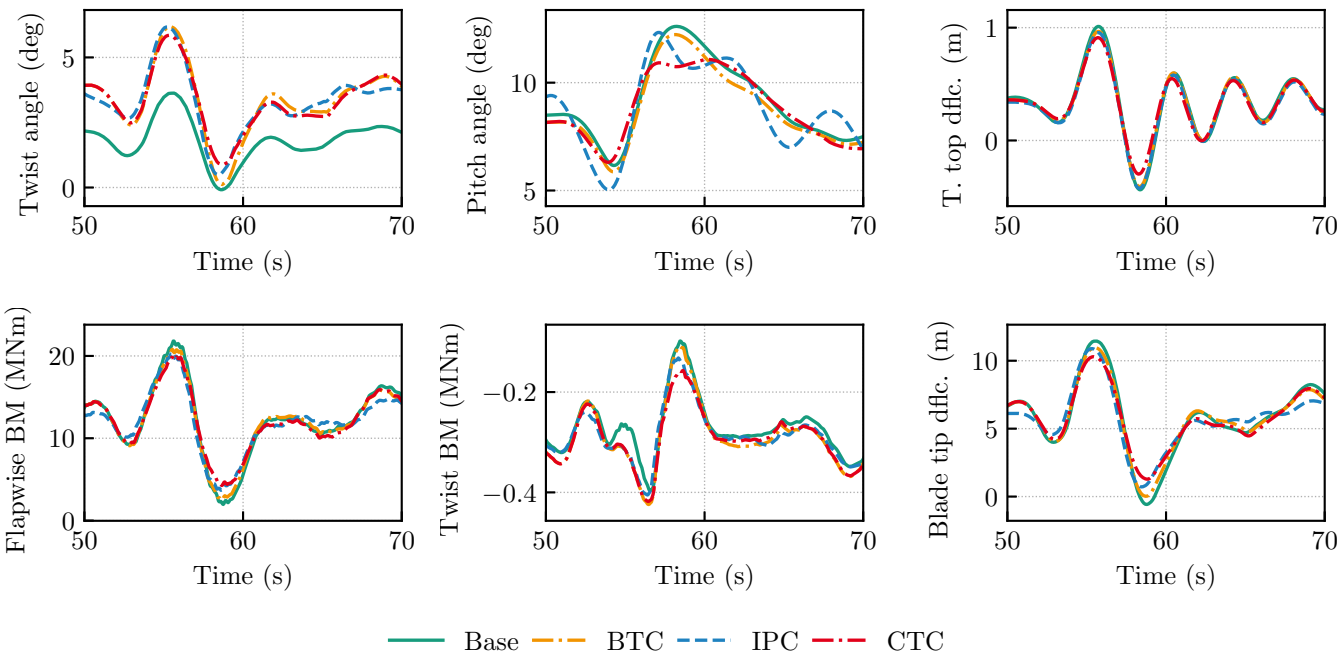

Fig. 4. Time domain representation of main wind turbines quantities for the investigated configurations. Wind profile is a extreme operating gust at 15 $^{m}/_{s}$. Tower is abbreviated with T.

compared to the Base case. Other differences compared to the passive use of BTC are insignificant. The blade root twist moment is increased by 1 % for BTC and CTC. Only IPC reduces all blade fatigue loads by significant amounts. Overall, the positive effects of BTC for fatigue loads remain when CTC is active. A main benefit results from the BTC blade, which reduces the DEL for the flap-wise bending moment by 5 %. It is clearly visible that IPC has a high impact on fatigue load reduction in combination with BTC. The flap-wise bending moment and the root twist moment are reduced by 30 % and 10 %, respectively.

Table 2. Changes relative to Base configuration for DEL and energy produced for turbulent wind

Load	BTC	IPC	CTC
Blade root edge-wise moment	1.00	0.95	1.00
Blade root flap-wise moment	0.95	0.70	0.95
Blade root twist moment	1.01	0.90	1.01
Hub force fore-aft	0.96	0.96	0.97
Hub force side-side	1.01	1.02	1.01
Tower bottom fore-aft BM	1.01	1.04	1.01
Tower bottom side-side BM	0.99	1.01	0.99
Energy	0.97	0.97	0.97

The combination of BTC and IPC is able to reduce the fatigue loads, while CTC is capable of decreasing the range between minimum and maximum load the most, which minimizes the sudden change of the load level. All configurations show a energy loss of 3 %.

4. DISCUSSION

Active control methods improve the benefits of BTC. Maximum load reduction is achieved, by the suggested feedforward controller using the twist rate as a gust detection. The main benefits are found for flap-wise loads, blade tip deflection and and tower top acceleration, which leads to reduced bending moments at the tower bottom. The only drawback is found for the blade root twist moment, but the CTC shows the lowest increase. In accordance with the literature, the simulations show a benefit of using BTC rotor blades. In particular, the combination of BTC and IPC shows synergistic load reduction, which matches the results from Bottasso et al. (2012).

The loss in energy production found in simulations with turbulent wind is ascribed to the design of the swept blade. This design is only optimized for loads and not for energy production. Compensation of the energy loss is expected by a change of the blade pre-twist, which requires a more refined aerodynamic design and was thus not considered within the scope of this controls-oriented paper. The control methods do not affect the energy production. Furthermore, the robustness of the system has to be evaluated. It is assumed, that the twist rate is perfectly known. In reality the measurements would be noisy and are probably not accurate. Currently, commercially available wind turbines are not equipped with sensors that measure the twist angle, but it was shown that is is well possible to determine it using more advanced measurement techniques (Meyer (2018)).

5. CONCLUSION

A novel method (Collective Twist Control) for mitigation of gust effects has been presented. The feedforward of the blade tip twist rate establishes a fast gust detection and the pitch angle can be adjusted accordingly. The simulations demonstrated that this novel control strategy can lead to the reduction of maximum loads during gust events. Additionally, blade tip movement can be reduced by BTC blades using active control methods. This will

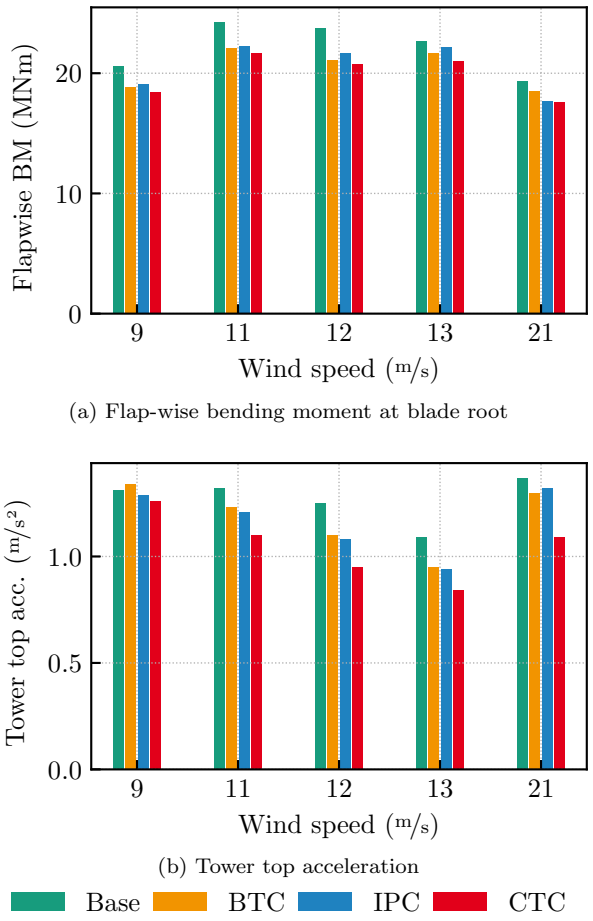

(a) Flap-wise bending moment at blade root

(b) Tower top acceleration

Fig. 5. Maximum loads during EOG at various wind speeds for the different configurations. The label order in the legend is the same as in the bar plot

become important as modern rotor blades become larger and more flexible. Additionally, simultaneous use of IPC and CTC can be tested to combine the load reduction of fatigue and maximum loads. It was shown that CTC is effective for BTC blades, however the effect of CTC applied to straight blades could also lead to reduction of maximum loads.

REFERENCES

Bossanyi, E.A. (2003). Wind Turbine Control for Load Reduction. *Wind Energy*, 6(3), 229–244.

Bottasso, C.L., Campagnolo, F., Croce, A., and Tibaldi, C. (2012). Optimization-based study of bend-twist coupled rotor blades for passive and integrated passive/active load alleviation. *Wind Energy*, 2, 1149–1166.

Burton, T., Jenkins, N., Sharpe, D., and Bossanyi, E. (2011). *Wind Energy Handbook*. John Wiley & Sons, Hoboken, 2nd ed. edition.

IEC (2019). IEC 61400-1: Wind Turbines - Part 1: Design Requirements.

Jonkman, B.J. (2009). TurbSim User's Guide: Version 1.50.

Kallesøe, B.S. (2011). Effect of steady deflections on the aeroelastic stability of a turbine blade. *Wind Energy*, 14(2), 209–224.

Leimeister, M. and Thomas, P. (2017). The OneWind Modelica Library for Floating Offshore Wind Turbine Simulations with Flexible Structures. In *Proceedings of the 12th International Modelica Conference*, 633–642. Linköping Electronic Conference Proceedings.

Liu, C., Li, Y., Cooney, J.A., Fine, N.E., and Rotea, M.A. (2018). NREL Fast Modeling for Blade Load Control with Plasma Actuators. In *IEEE Conference on Control Technology and Applications*, 1644–1649. IEEE.

Manolas, D.I., Serafeim, G.P., Chaviaropoulos, P.K., Riziotis, V.A., and Voutsinas, S.G. (2018). Assessment of load reduction capabilities using passive and active control methods on a 10MW-scale wind turbine. *Journal of Physics: Conference Series*, 1037, 032042.

Meng, F., Wenske, J., and Gambier, A. (2016). Wind turbine loads reduction using feedforward feedback collective pitch control based on the estimated effective wind speed. In *American Control Conference*, 2289–2294. IEEE.

Meyer, T.e.a. (2018). Nutzung von Inertialmesstechnik zur Stützung modellbasierter Berechnungsalgorithmen von Windenergieanlagen. *VDI-Berichte*, (2324), 51–62.

Navalkar, S.T., van Wingerden, J.W., van Solingen, E., Oomen, T., and van Kuik, G. (2014). Subspace Predictive Repetitive Control for wind turbine load alleviation using trailing edge flaps. In *American Control Conference*, 4422–4427. IEEE.

Njiri, J.G. and Söffker, D. (2016). State-of-the-art in wind turbine control: Trends and challenges. *Renewable and Sustainable Energy Reviews*, 60, 377–393.

Popko, W., Thomas, P., Sevinc, A., Rosemeier, M., Bätge, M., Braun, R., Meng, F., Horte, D., and Balzani, C. (2018). IWES Wind Turbine IWT-7.5-164. Rev 4. Bremerhaven.

Stäblein, A.R., Hansen, M.H., and Pirrung, G. (2017a). Fundamental aeroelastic properties of a bend–twist coupled blade section. *Journal of Fluids and Structures*, 68, 72–89.

Stäblein, A.R., Hansen, M.H., and Verelst, D.R. (2017b). Modal properties and stability of bend–twist coupled wind turbine blades. *Wind Energy Science*, 2(1), 343–360.

Sutherland, H.J. (1999). On the Fatigue Analysis of Wind Turbines. Albuquerque, New Mexico.

Teßmer, J., Icpinar, C., Riemenschneider, J., Daniele, E., Balzani, C., Sevinc, A., and Hölling, M. (2016). Schlussbericht SB: Smart Blades : 01.12.2012-30.04.2016. Braunschweig.

Thomas, P., Gu, X., Samlaus, R., Hillmann, C., and Wihlfahrt, U. (2014). The OneWind Modelica Library for Wind Turbine Simulation with Flexible Structure - Modal Reduction Method in Modelica. In *Proceedings of the 10th International Modelica Conference*, Linköping Electronic Conference Proceedings, 939–948. Linköping University Electronic Press.

van Kuik, G. A. M. et al. (2016). Long-term research challenges in wind energy – a research agenda by the European Academy of Wind Energy. *Wind Energy Science*, 1(1), 1–39.

Verelst, D.R.S. and Larsen, T.J. (2010). *Load consequences when sweeping blades - a case study of a 5 MW pitch controlled wind turbine*, volume 1724 of *Risø R, Report*. Risø National Laboratory, Roskilde.